Clinical Cancer Research

Cancer-Associated Fibroblasts Affect Intratumoral CD8$^+$ and FoxP3$^+$ T Cells Via IL6 in the Tumor Microenvironment

Takuya Kato[1], Kazuhiro Noma[1], Toshiaki Ohara[1,2], Hajime Kashima[1], Yuki Katsura[1], Hiroaki Sato[1], Satoshi Komoto[1], Ryoichi Katsube[1], Takayuki Ninomiya[1], Hiroshi Tazawa[1,3], Yasuhiro Shirakawa[1], and Toshiyoshi Fujiwara[1]

Abstract

Purpose: Cancer-associated fibroblasts (CAFs) in the tumor microenvironment (TME) play a central role in tumor progression. We investigated whether CAFs can regulate tumor-infiltrating lymphocytes (TILs) and their role in tumor immunosuppression.

Experimental Design: A total of 140 cases of esophageal cancer were analyzed for CAFs and CD8$^+$ or forkhead box protein 3 (FoxP3$^+$) TILs by IHC. We analyzed cytokines using murine or human fibroblasts and cancer cells. Murine-derived fibroblasts and cancer cells were also inoculated into BALB/c or BALB/c-*nu/nu* mice and the tumors treated with recombinant IL6 or anti-IL6 antibody.

Results: CD8$^+$ TILs and CAFs were negatively correlated in intratumoral tissues ($P < 0.001$), whereas FoxP3$^+$ TILs were positively correlated ($P < 0.001$) in esophageal cancers. Cocultured Colon26 cancer cells and fibroblasts resulted in accelerated tumor growth in BALB/c mice, along with decreased CD8$^+$ and increased FoxP3$^+$ TILs, compared with cancer cells alone. *In vitro*, IL6 was highly secreted in both murine and human cancer cell/fibroblast cocultures. IL6 significantly increased Colon26 tumor growth in immune-competent BALB/c ($P < 0.001$) with fewer CD8$^+$ TILs than untreated tumors ($P < 0.001$), whereas no difference in BALB/c-*nu/nu* mice. In contrast, FoxP3$^+$ TILs increased in IL6-treated tumors ($P < 0.001$). IL6 antibody blockade of tumors cocultured with fibroblasts resulted not only in regression of tumor growth but also in the accumulation of CD8$^+$ TILs in intratumoral tissues.

Conclusions: CAFs regulate immunosuppressive TIL populations in the TME via IL6. IL6 blockade, or targeting CAFs, may improve preexisting tumor immunity and enhance the efficacy of conventional immunotherapies. *Clin Cancer Res; 24(19); 4820–33. ©2018 AACR.*

Introduction

Esophageal cancer is known as one of the most aggressive malignant tumors, frequently showing lymph node metastasis and tumor invasion into adjacent organs, even in the early stages. The 5-year survival rate for esophageal cancer remains only 16.9%, even with current advanced modalities (1). The development of novel therapeutic approaches is thus essential in order to improve the prognosis of patients suffering from this disease. Esophageal cancer is a carcinoma with one of the largest numbers of neoantigens and is likely to benefit from immunotherapy approaches in the near future (2–4).

Recently, the technological innovation of targeted immunotherapy has dramatically improved the prognosis of cancer patients (5–8). Immune checkpoint inhibitors have already been applied to the treatment several malignancies (8), with some reports of favorable outcomes. Furthermore, recent new gene engineering approaches for the modification of tumor-specific T-cell function, such as the production of chimeric antigen receptor (CAR) T cells, have been introduced, and there is considerable expectation surrounding this innovation (9, 10). However, there are many problems that remain to be solved with regard to T-cell–mediated immunotherapies (11, 12). The ratio of responders has so far been limited, and although the precise mechanism is not yet clear (13), the tumor microenvironment (TME) has been strongly implicated in determining outcomes (14–17). It is currently thought that the TME strongly affects tumor immunosuppression (18), as it is composed of immune cells, tumor vasculature, and cancer-associated fibroblasts (CAFs; ref. 19). CAFs are the most abundant cell population in the TME, and are thus thought to play an essential role in tumor immunosuppression (20–22). They are generally defined as activated fibroblasts within the TME that promote tumor progression and therapeutic resistance (23–25). Several recent reports have shown that CAFs regulate tumor-infiltrating lymphocytes (TILs) via CXCL12 signaling and recruitment of myeloid-derived suppressor cells

[1]Department of Gastroenterological Surgery, Okayama University Graduate School of Medicine, Dentistry and Pharmaceutical Sciences, Okayama, Japan. [2]Department of Pathology & Experimental Medicine, Okayama University Graduate School of Medicine, Dentistry and Pharmaceutical Sciences, Okayama, Japan. [3]Center for Innovative Clinical Medicine, Okayama University Hospital, Okayama, Japan.

Note: Supplementary data for this article are available at Clinical Cancer Research Online (http://clincancerres.aacrjournals.org/).

Corresponding Author: Kazuhiro Noma, Department of Gastroenterological Surgery, Okayama University Graduate School of Medicine, Dentistry, and Pharmaceutical Sciences, 2-5-1 Shikata-cho, Kita-ku, Okayama 700-8558, Japan. Phone: 81-86-235-7255; Fax: 81-86-221-8775; E-mail: knoma@md.okayama-u.ac.jp

doi: 10.1158/1078-0432.CCR-18-0205

Translational Relevance

Despite dramatic improvement of clinical outcomes by innovation of T-cell–mediated immunotherapies, the clinical response can be strongly associated with the immunosuppressive tumor microenvironment (TME). Here, we show that cancer-associated fibroblasts (CAFs) regulate tumor-infiltrating lymphocytes (TIL) and change the T-cell populations. Intratumoral $CD8^+$ and $FoxP3^+$ TILs are independent prognostic factors in esophageal cancer and CAFs affect the distribution of TILs. *In vitro*, CAFs activated by cancer cells secrete high levels of IL6. *In vivo*, CAFs accelerate tumor growth in immune-competent mice, along with phenotypic changes in T-cell populations, decreased $CD8^+$ and increased $FoxP3^+$ TILs. Moreover, the accelerated tumor growth observed in CAF cocultures is significantly reduced by IL6 blockade; therefore, the immunosuppressive TIL population is improved. CAFs may be a biomarker of immunosuppressive TME. IL6 blockade or targeting CAFs may improve preexisting tumor immunity and enhance the efficacy of conventional immunotherapies.

(MDSC; refs. 15, 26, 27). Therefore, the importance of the relationship between CAFs and tumor immunosuppression cannot be understated, and it is an area that requires further research.

In contrast, TILs represent the host immune response to tumor proliferation and metastasis (2, 28). $CD8^+$ T cells, which are cytotoxic T lymphocytes (CTLs), demonstrate cytotoxic activity toward tumor cells by triggering apoptosis, and are considered to be the frontline defense against cancer (29–32). Several recent clinical studies have evaluated the role of TILs as prognostic and predictive factors (11), and have shown that $CD8^+$ TILs are associated with longer disease-free survival (DFS) and overall survival (OS) in colon and ovarian carcinoma. Meanwhile, forkhead box protein 3-positive ($FoxP3^+$) TILs, which are regulatory T cells (Tregs), are thought to suppress mainly antitumor immunity and immunotherapy, as they effectively suppress the proliferation and activation of CTL (30–32). It is reported that $FoxP3^+$ TILs are associated with worse prognosis in breast cancer, gastric cancer, and melanoma (29–33). Furthermore, in esophageal cancer, it has been reported that a stratification based on PD-L1 expression and $CD8^+$ TIL status is associated with overall survival (34). However, the role of these TIL populations remains controversial in esophageal cancer (35–38). Moreover, T-cell infiltration into inflamed tissues is a multistep process involving tethering/rolling, activation, adhesion, and transmigration, but it is not fully understood how T-cell trafficking and infiltration is regulated in the immune-suppressive TME (13, 17, 18, 39). The role of TME stromal cells, especially CAFs, has now become a major focus in this regard (15, 18, 26).

In this study, we hypothesized that CAFs are implicated in the immunosuppression of esophageal tumors, especially with regard to $CD8^+$ and $FoxP3^+$ TILs, and are thus important for patient prognosis. We therefore performed clinicopathological analysis using primary tissue samples, verified whether CAFs affect tumor immunosuppression using an *in vivo* model, and further explored the mechanisms underpinning these interactions *in vitro*.

Materials and Methods

Patients and clinical information

A total of 149 patients who received radical surgery for esophageal cancer in the Department of Gastroenterological Surgery at Okayama University Hospital between 2008 and 2010 were registered for this study. Patients who had received endoscopic mucosal resection (EMR) or endoscopic submucosal dissection (ESD) followed by surgery, who were diagnosed with melanoma or a distant metastasis, or who had no tumor presence/complete response after neo-adjuvant therapy were excluded. In total, 140 samples were finally analyzed. All patients were reviewed for age, sex, histologic type, neoadjuvant therapy, pathologic invasion depth (pT), and lymph node status (pN). Tumor classification was applied according to TNM Classification of Malignant Tumors 7th edition (UICC 7th edition).

Mice and cell lines

Athymic female nude mice (BALB/c-*nu*/*nu*), female BALB/c mice, and female C57BL/6 mice were purchased from Clea. Animals were maintained in specific pathogen-free conditions in the animal laboratory at Okayama University. Protocols were approved by the Ethics Review Committee for Animal Experimentation of Okayama University, Okayama, Japan. The murine cell lines of colon cancer (Colon26), luciferase-expressing colon cancer (Colon26-luc), and breast cancer (4T1), as well as the murine fibroblast lines (NIH/3T3, BALBc/3T3, and MEF), were purchased from the Japanese Collection of Research Bioresources (JCRB) Cell Bank (Osaka, Japan). The murine cell line of squamous cell carcinoma (SCCVII) was kindly provided by Professor Yuta Shibamoto (Department of Quantum Radiology, Nagoya City University, Nagoya, Japan), and pancreatic ductal adenocarcinoma (Pan02) was obtained from the National Cancer Institute at Frederick (MD, USA). Human cell lines of esophageal squamous cell cancer (TE4), breast cancer (MCF-7), pancreatic ductal adenocarcinoma (Panc-1), and colon cancer (DLD-1) were also purchased from JCRB. The primary human esophageal fibroblasts, designated FEF3, were isolated from human fetal esophagus as described previously (24). The normal lung fibroblast line NHLF was purchased from Cambrex Corporation and WI-38 fetal lung human fibroblast was purchased from the Health Science Research Resource Bank (Osaka, Japan).

IHC for CD8, FoxP3, and alpha smooth muscle actin (αSMA) in clinical specimens

Tissue blocks of formalin-fixed and paraffin-embedded surgical specimens of esophageal cancer were sectioned into 2-μm slices for IHC. First, the presence of tumor was confirmed using hematoxylin and eosin (HE) stain. Sectioned tissues were then deparaffinized and soaked in 0.3% H_2O_2 in methanol at room temperature (RT) for 10 minutes to extinguish endogenous peroxidase activity. Antigen retrieval was performed by heating specimens in a sodium citrate buffer solution using a microwave. After cooling, sections were incubated in Peroxidase Blocking Reagent (Dako) for 10 minutes at RT. Sectioned tissues were incubated with primary antibody against CD8 (Dako, clone C8/144B, 1:100 dilution) or FoxP3 (Abcam, ab20034, clone 236A/E7, 1:100 dilution) or αSMA (SIGMA, A2547, clone 1A4, 1:1,000 dilution) for 30 minutes at RT. Following three 5-minute washes with PBS, sections were incubated with antimouse secondary antibody for 30 minutes at RT. After washing, the enzyme substrate

3,3′-diaminobenzidine (Dako) was used for visualization, and sections were counterstained with Meyer's hematoxylin.

Immunofluorescence microscopy for CD8, FoxP3, and αSMA in clinical specimens

Slides were deparaffinized and washed, then protein blocking was carried out at RT for 10 minutes. The primary antibody against αSMA conjugated to FITC (Abcam, ab8211, clone 1A4, 1:100 dilution) was added at 4°C overnight; antigen retrieval was performed in the dark as described above. Primary antibodies against CD8 or FoxP3 were added as described above, at RT for 30 minutes. The secondary antibody Alexa Fluor 568 was added at RT for 1 hour. Coverslips were covered with a drop of mounting medium (Vector Laboratories, H-1200) and were subsequently photographed using a fluorescence microscope (BZ-X700; Keyence).

Immunofluorescence microscopy for αSMA in cultured cells

NIH/3T3 fibroblasts were seeded onto four-chamber glass slides and cultured in DMEM containing 10% FBS or conditioned medium from Colon26 cells for 96 hours. NIH/3T3 cells were fixed with 4% paraformaldehyde and permeabilized with methanol. Slides were stained with the primary antibody against αSMA (Abcam, ab5694, 1:250 dilution) overnight at 4°C. The secondary antibody Alexa Fluor 568 was added at 4°C for 1 hour. Slides were covered and photographed using a Confocal Laser Scanning Biological Microscope (FV10i; Olympus).

Quantitation of TILs and evaluation of αSMA area index

First, tumor boundaries were confirmed by H&E staining under microscopy at low magnification (10× objective lens). Next, the slides were examined at high magnification (40× objective lens), and four nonoverlapping fields with abundant $CD8^+$ or $FoxP3^+$ TILs were selected from each of the intratumoral or the peritumoral tissues. The number of TILs was counted using Image J software (http://rsb.info.nih.gov/ij/) and the intratumoral or peritumoral tissues were recorded separately. CAFs were defined as fibroblasts expressing αSMA, and αSMA scoring was evaluated using an "Area Index," calculated by ImageJ. To ensure that the whole tumor was evenly evaluated, at least four or more fields including stromal cells were carefully selected to evaluate CAFs. The mean value obtained from each sectioned tissue was defined as the αSMA area index. All evaluations were performed by an independent pathologist who was blinded to clinical information.

Western blotting

NIH/3T3 fibroblasts, stimulated with Colon26 cell conditioned medium for 96 hours, were examined for the expression of αSMA by Western blotting. Cells were homogenized and whole proteins extracted by centrifugation for 10 minutes at 4°C. Samples containing 30 mg of protein were separated by electrophoresis on a polyacrylamide gel. Proteins were transferred to membranes and probed overnight at 4°C with primary antibody (Abcam, ab5694, 1:500 dilution). Membranes were then washed in buffer and incubated with secondary antibodies for 1 hour at RT. After washing, membranes were visualized using LAS-4000 mini (FUJIFILM).

Quantification of IL6 by ELISA

Colon26 (2.5×10^4, 5.0×10^4, or 10×10^4 cells) or NIH/3T3 (5.0×10^4, 10×10^4, or 20×10^4 cells) were seeded and cultured in a T25 flask with 2% FBS in DMEM. Culture supernatants were collected 96 hours later. The level of IL6 in each supernatant was measured using the Quantikine ELISA mouse IL6 Immunoassay (R&D Systems). In coculture experiments, both cell types were seeded and cultured using the combinations of cell numbers described above. To evaluate the necessity of direct contact between cancer cells and fibroblasts, Falcon Cell Culture Inserts (Catalog No. 353090) and Falcon Companion TC Plates (Catalog No. 353502, six wells) were used. Colon26 (1.0×10^4 cells) or NIH/3T3 (2.0×10^4 or 4.0×10^4 cells) were seeded, respectively. Data are presented as IL6 levels per 1.0×10^5 cells. In addition, other cancer cells (5.0×10^4 of 4T1, SCCVII, or Pan02) and fibroblasts (10×10^4 of BALBc/3T3 or MEF) were cocultured and analyzed according to the same protocol. Finally, human cancer cells (5.0×10^4 of TE4, DLD-1, Panc-1, or MCF-7) and fibroblasts (10×10^4 of FEF3, WI-38, or NHLF cells) were also cocultured. For these experiments, supernatants were collected as described above and IL6 levels were measured using the Quantikine ELISA human IL6 Immunoassay (R&D Systems). Data are presented as IL6 levels per 1.0×10^5 cells.

In vivo experiments

To evaluate tumor immunosuppression by CAFs, we used 6-week-old female BALB/c-*nu/nu* and BALB/c mice. Mice were anesthetized and 150 μL of a single-cell suspension containing either Colon26-luc (0.25×10^6 cells) only, or Colon26-luc (0.25×10^6 cells) with NIH/3T3 fibroblasts (0.5×10^6 cells), was injected into the skin of the right flank. For analyzing tumor growth, mice were injected intraperitoneally with luciferin (VivoGlo Luciferin, In Vivo Grade) and imaged under isoflurane anesthesia 15 minutes later. Bioluminescence images were obtained with an IVIS Lumina imaging system (Xenogen IVIS Lumina II; Caliper Life Sciences), and image analysis and bioluminescent quantification were performed using Living Image software. This examination was performed every 4 days, from day 4 to day 16.

To investigate the effects of IL6, BALB/c, and BALB/c-*nu/nu* mice were injected with 1.0×10^6 Colon26 cells into the right flank. Subsequently, 200 ng/50 μL/body of recombinant mouse IL6 protein (R&D systems, 406-ML) or 50 μL of PBS was directly injected into the tumors every 3 days. Tumor volumes and mouse weights were also evaluated every 3 days. For other cancer models, C57BL/6 mice were inoculated with 1.0×10^6 Pan02 cells and were treated according to the same protocol. To explore immunosuppression by CAFs and improvement by IL6 blockade, 0.5×10^6 Colon26 cells alone (the Colon26 group) or 0.5×10^6 Colon 26 cells with 1.0×10^6 NIH/3T3 cells (the Colon26+NIH/3T3 group) were inoculated into the right flank of BALB/c mice. Mice in the Colon26+NIH/3T3 group were treated with 200 μg/body of isotype control (BD Bioscience; Catalog No. 559286) or anti-IL6 antibodies (BioXcell) by subcutaneous injection every 3 days. Tumor volumes and mouse weights were also evaluated every 3 days. All mice were euthanized after observation; subcutaneous tumors were then harvested and their tumor weights measured.

IHC of *in vivo*-derived tumor tissues

Harvested subcutaneous tumors were formalin-fixed and paraffin-embedded. Subsequent deparaffinization and antigen-retrieval were performed, as described above. Primary antibodies against CD8a (eBioscience, clone 4SM15, 1:100 dilution), FoxP3 (eBioscience, clone FJK-16s, 1:100 dilution), and αSMA (SIGMA, clone 1A4, 1:1,000 dilution) were added and incubated for

60 minutes at RT. Primary antibody against IL6 (Abcam; Catalog No. ab6672, 1:500 dilution) was added and incubated overnight at 4°C, and after washing, secondary antibody was added and incubated for 30 minutes at RT. Sections were visualized and counterstained, as described above. Counting of $CD8^+$ and $FoxP3^+$ TILs and evaluation of αSMA and IL6 area index were performed using ImageJ software, as described above.

Statistical analysis

All statistical analysis was performed with the SPSS advanced statistics 19.0 software (SPSS). For $CD8^+$ or $FoxP3^+$ TIL counts and the area index of αSMA, cutoffs were defined using the median value of the high or low groups. OS and DFS were calculated using the Kaplan–Meier method, with the log-rank test used to compare between subgroups. HRs and 95% confidence intervals (CIs) for clinical variables were calculated using Cox proportional hazards regression in univariate and multivariate analysis. Spearman's correlation was used to assess the relationship between TIL counts and the area index of αSMA. For two-group comparisons, the Mann–Whitney test or unpaired *t* test was used. For multiple-group comparisons, ANOVA with Tukey test was used. *P* values < 0.05 were considered statistically significant.

Study approval

This study was performed in accordance with the ethical standards of the Helsinki Declaration and the ethical guidelines for Medical and Health Research Involving Human Subjects (40). All cases were de-identified and details have been removed from their case descriptions to ensure anonymity. The outline of our study was published on our web page to explain the study, and also to provide opportunities for disagreement. Because of its retrospective nature, we requested and were granted waivers of informed consent from the ethics committee. This study was approved and reviewed by the Ethics Review Board of Okayama University (No. 1603-023; Okayama, Japan). Mouse experiments were performed in a specific pathogen-free environment at the Okayama University animal facility according to institutional guidelines, and all animal experimental protocols were approved and reviewed by the Ethics Review Committee for Animal Experimentation of Okayama University. All experiments were performed in accordance with the guidelines and regulations indicated by these committees.

Results

CAFs affect the distribution of TILs in esophageal cancer tissue

To explore the distribution of $CD8^+$ and $FoxP3^+$ TILs in esophageal cancer, we conducted IHC using surgically resected tissues. There were differences in accumulation of TILs between intra- and peritumoral sites, as demonstrated by the fact that $CD8^+$ TILs were found in greater numbers in peritumoral than intratumoral tissues (Fig. 1A), and a similar trend was observed for $FoxP3^+$ TILs (Fig. 1B). These results raise the possibility that the migration of lymphocytes into intratumoral sites is affected by stromal cells in the TME. Next, we evaluated the distribution of CAFs, which were identified as stromal cells expressing αSMA (Fig. 1C and D). In intratumoral tissues, the presence of CAFs was highly variable; in contrast, in peritumoral tissues, CAFs were generally present at relatively low numbers. To explore the relationship between the distribution of TILs and CAFs, we performed immunofluorescence (IF) imaging using anti-αSMA (green), and anti-CD8 or anti-FoxP3 (red) antibodies. Costaining of anti-αSMA and anti-CD8 revealed that numerous $CD8^+$ TILs were present in both intratumoral and peritumoral sites when CAFs were in low numbers. In contrast, in cases where CAFs were present at high numbers (the majority of stromal fibroblasts staining green), $CD8^+$ TILs in the intratumoral tissues were scarce, despite an accumulation of $CD8^+$ TILs in peritumoral sites (Fig. 1E). Unlike $CD8^+$ TILs, $FoxP3^+$ TILs were found at higher numbers in intratumoral sites in high-CAF cases compared with low-CAF cases (Fig. 1F). Thus, CAFs may influence tumor immunosuppression by regulating the migration or invasion of TILs.

Intratumoral $CD8^+$ and $FoxP3^+$ TILs are independent prognostic factors for esophageal cancer

To investigate the clinical impact of TILs in esophageal cancer, we evaluated their association with prognosis in 140 consecutively-enrolled cases of esophageal cancer. The number of $CD8^+$ or $FoxP3^+$ lymphocytes was counted in four sites for each intratumoral or peritumoral tissue (Fig. 2A) using IHC (Fig. 2B, left), and the average calculated (Fig. 2B, right). The number of both $CD8^+$ and $FoxP3^+$ TILs in peritumoral sites was thus significantly higher than in intratumoral tissues.

Next, we evaluated the relationship between $CD8^+$ and $FoxP3^+$ TIL distribution, clinicopathologic features, and clinical outcome. Tumor depth, lymph node status, and neo-adjuvant therapy status were found to be significant prognostic factors for OS by univariate analysis ($P < 0.001$ for all; Supplementary Tables S1 and S2). Furthermore, patients with high $CD8^+$ TIL numbers in intratumoral sites had significantly longer OS than those with low numbers. However, the high $FoxP3^+$ TIL group for intratumoral tissues had significantly a shorter OS (Fig. 2C). However, in peritumoral tissues, no significant correlations between $CD8^+$ or $FoxP3^+$ TIL numbers and prognosis were identified (Fig. 2D). In the stage-related subgroup analysis for OS in intratumoral tissues, higher $CD8^+$ or lower $FoxP3^+$ TIL numbers tended to reflect better OS for all Stages (Supplementary Fig. S1; Supplementary Table S3). Moreover, in multivariate analysis, both $CD8^+$ and $FoxP3^+$ TILs were independent prognostic factors for OS ($CD8^+$; HR = 0.45, 95% CI, 0.27–0.77, $P = 0.004$; $FoxP3^+$, HR = 1.86, 95% CI, 1.05–3.29, $P = 0.034$; Supplementary Table S4). Similar trends were demonstrated for DFS (Supplementary Tables S2–S4). Thus, in intratumoral but not peritumoral sites, both $CD8^+$ and $FoxP3^+$ TILs strongly contribute to esophageal cancer prognosis.

Correlation between CAFs and $CD8^+$/$FoxP3^+$ TIL distribution in intratumoral tissues

To confirm the correlation between CAFs and $CD8^+$/$FoxP3^+$ TIL distribution in esophageal cancer, we evaluated the presence of CAFs expressing αSMA in each sample using IHC. The mean value was calculated as an "αSMA area index" (Fig. 3A). In intratumoral tissues, a negative correlation between $CD8^+$ TILs and CAFs was demonstrated in scatter plots ($r = -0.416$), and a positive correlation between $FoxP3^+$ TILs and CAFs was also observed ($r = 0.484$; Fig. 3B). Furthermore, in a comparison based on αSMA area index, those with a high αSMA area index (i.e., CAF-rich cases) showed significantly lower $CD8^+$ and higher $FoxP3^+$ TIL numbers in intratumoral tissues (CD8+, $P < 0.001$; FoxP3+, $P < 0.001$; Fig. 3C). In contrast, in peritumoral tissues, no significant correlation was observed.

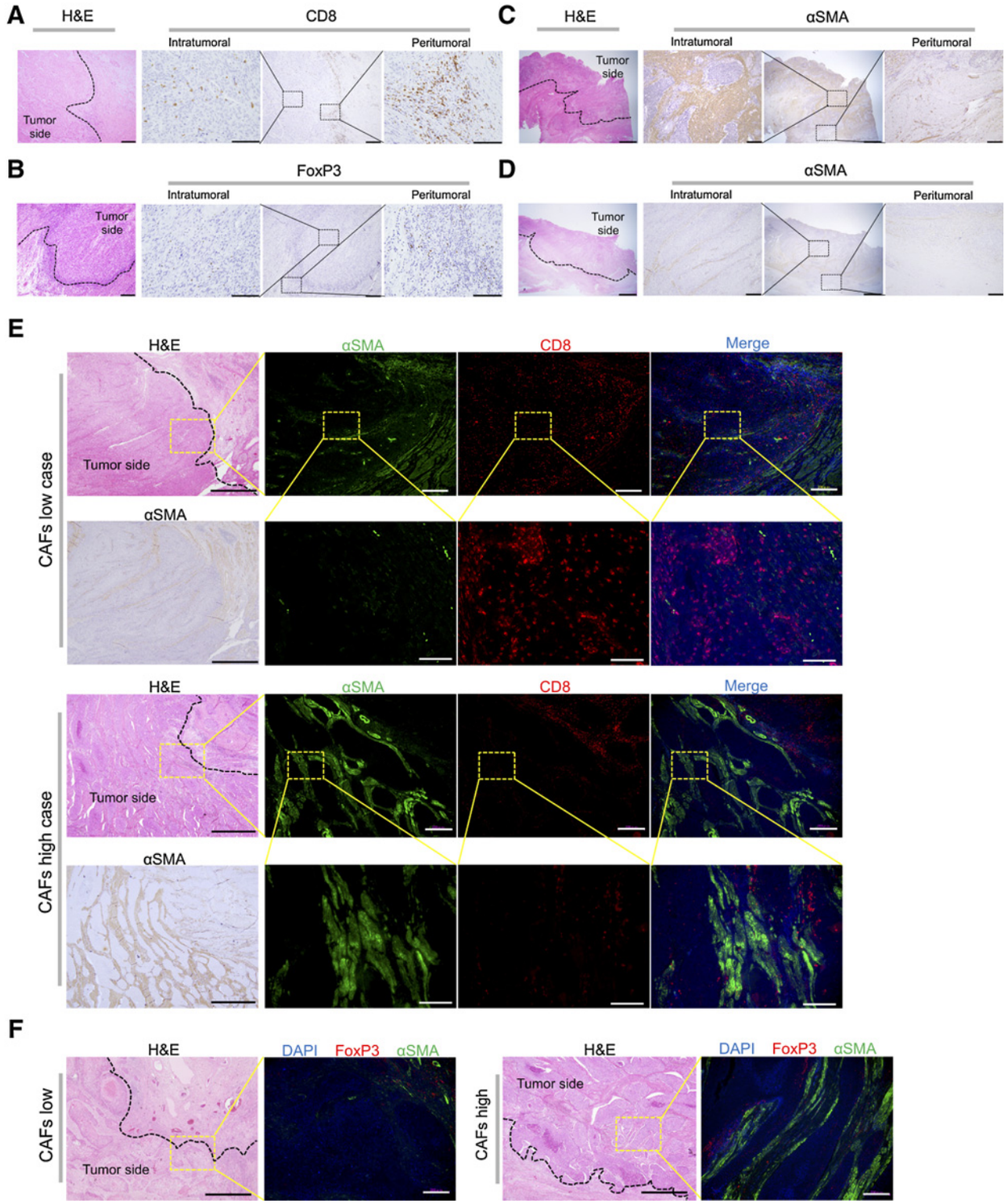

Figure 1.

Relative distribution of TILs and CAFs in surgically resected human esophageal cancer samples. **A,** IHC for CD8-expressing T cells is shown at low and high magnification (40× and 400×). The distribution of $CD8^+$ TILs is different between intratumoral and peritumoral tissue. **B,** IHC for FoxP3 expression is shown. **A** and **B,** Scale bars: 1 mm (HE, 40×), 100 μm (400×). **C** and **D,** IHC for αSMA^+ CAFs shows a variable distribution in intratumoral tissue between different cases, but no differences for peritumoral tissues. Scale bars: 2 mm (HE, IHC: 20 ×), 200 μm (100 ×). **C,** Representative example of a high-αSMA case. **D,** Representative example of a low-αSMA case. **E** and **F,** Double staining immunofluorescence (IF) images of CD8- or FoxP3-expressing lymphocytes and αSMA at middle and high magnification (100× and 400×). Scale bars: 1 mm (HE, IHC: 40×), 200 μm (100×), 50 μm (400×). **E,** $CD8^+$ TILs in intratumoral tissues are present at high numbers in a low-CAF case and at low numbers in a high-CAF case. **F,** In contrast, $FoxP3^+$ TIL numbers in intratumoral tissues are high in a high-CAF case and low in a low-CAF case.

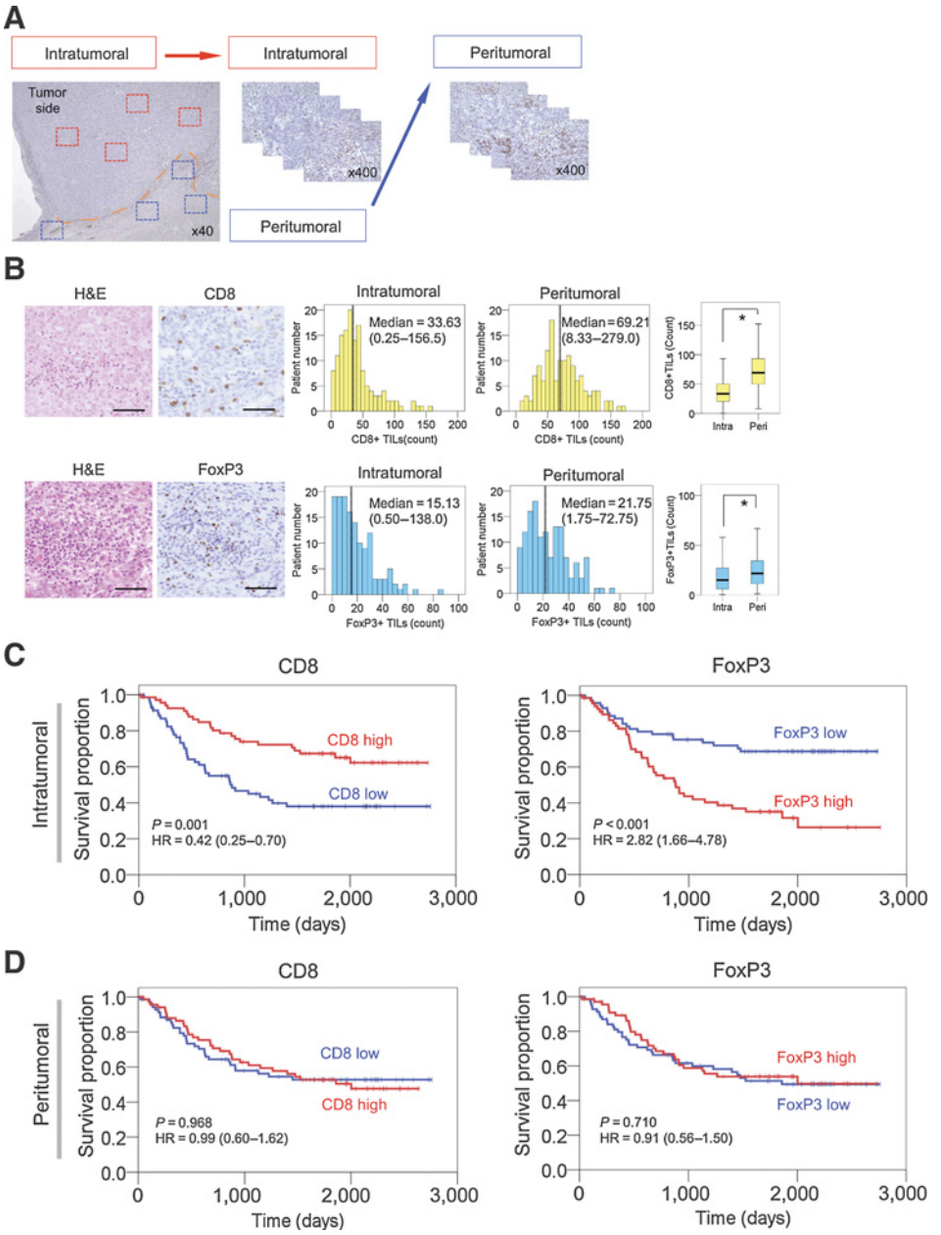

Figure 2.

Correlation between $CD8^+$ and $FoxP3^+$ TIL distribution and clinical outcome in 140 cases of esophageal cancer. **A,** Protocol for area selection. The intra-/peritumoral border was first defined at low magnification (40×). Four areas with the most abundant lymphocytes under high magnification (400×) were then selected for both intra- and peritumoral sites in each specimen. **B,** The average number of $CD8^+$ or $FoxP3^+$ TILs was recorded using ImageJ ($n = 140$ per group; black bar indicates median). $CD8^+$ and $FoxP3^+$ TILs in peritumoral tissues were more numerous than in intratumoral sites ($CD8^+$, $P < 0.001$; $FoxP3^+$, $P = 0.034$; Student t test). Scale bars: 50 μm. **C,** OS curves according to $CD8^+$ and $FoxP3^+$ TIL number (high or low groups) in intratumoral tissues. The $CD8^+$ high group showed significantly better prognosis, whereas the $FoxP3^+$ high group showed significantly worse prognosis (Cox regression hazard model, 95% confidence intervals, and log-rank test). **D,** Survival curves for TIL distribution in peritumoral tissues. No significant difference in outcome was detected for the high/low groups of $CD8^+$ and $FoxP3^+$.

Next, we evaluated the ratio of peri- to intratumoral $CD8^+$ TILs and identified lower, inter, and upper quartiles using box-and-whisker plots (Fig. 3D, left). We then compared the αSMA area index in each group (Fig. 3D, middle and right), finding that the αSMA area index in the upper quartile of the peri-/intratumoral $CD8^+$ TIL ratio was significantly higher than in other groups. It therefore appeared that CAFs strongly affected the distribution of $CD8^+$ TILs in these cases, resulting in lower $CD8^+$ TIL numbers in the intratumoral sites. In contrast, in the $FoxP3^+$ TIL analysis, the αSMA area index in the upper quartile group was significantly lower than other groups (Fig. 3E), suggesting that CAFs also accelerate the migration of $FoxP3^+$ lymphocytes into the intratumoral tissues. Furthermore, in $CD8^+$ TILs, a positive correlation between peri-/intratumoral ratios and CAFs was demonstrated in scatter plots ($r = 0.451$), and a negative correlation was also observed in $FoxP3^+$ TILs ($r = -0.448$; Supplementary Fig. S2). Taken together, these data provide strong evidence that esophageal cancer CAFs restrict the infiltration of $CD8^+$ TILs into intratumor tissues, and in contrast, promote the infiltration of $FoxP3^+$ TILs.

CAFs promote tumor immunosuppression *in vivo*

To further evaluate the relationship between CAFs and immunosuppression, *in vivo* experiments were performed using two types of mice, namely BALB/c and BALB/c-*nu/nu* mice. We used the luciferase-expressing mouse-derived cell line, Colon26-luc for these experiments. We established two groups, cancer cells alone (Colon26-luc) and cancer cells co-cultured with fibroblasts (Colon26-luc+NIH/3T3). Cancer cells and fibroblasts were subcutaneously inoculated into each mouse, and tumor growth was

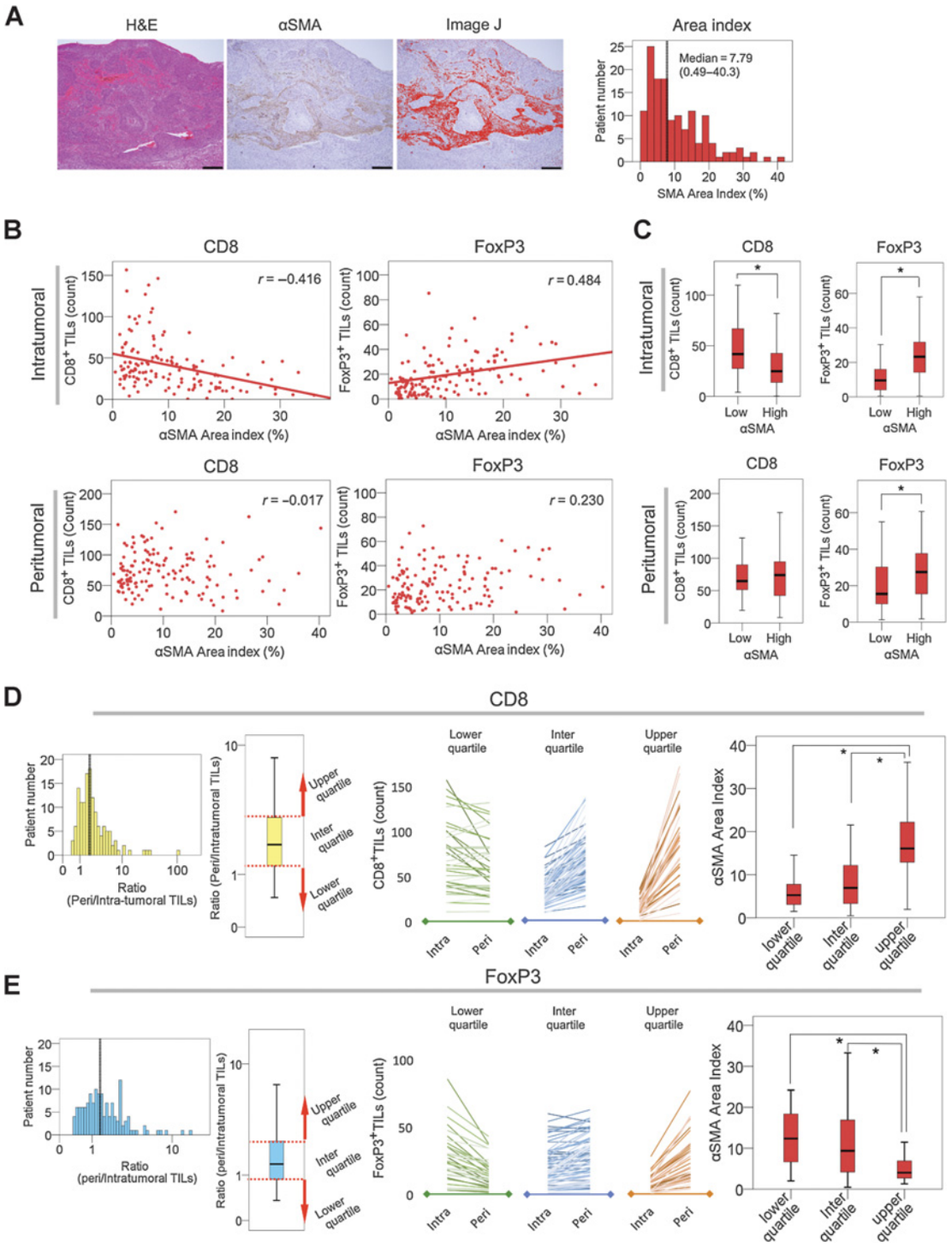

Figure 3.

Correlation of CAFs and CD8$^+$/FoxP3$^+$ TIL distribution in esophageal cancer tissues. **A,** Tissue staining with H&E and anti-αSMA, with the emphasis figure from ImageJ demonstrating the evaluation of area index. The mean of area ratio measurements was calculated as the αSMA area index; the αSMA area index for all cases is plotted as a histogram (black bar, median value). Scale bars: 200 μm. **B,** The correlation between CAFs and CD8$^+$ or FoxP3$^+$ TILs is shown by scatter plot. In intratumoral tissues, there was a negative correlation with CD8$^+$ TILs ($r = -0.416$), whereas there was a positive correlation for FoxP3$^+$ TILs ($r = 0.484$). No correlation was observed in peritumoral tissues (CD8$^+$, $r = 0.017$; FoxP3$^+$, $r = 0.230$; Spearman's coefficient). **C,** Comparisons based on high or low αSMA area index are shown by the box and whisker plots. In intratumoral tissues, significant differences were observed (CD8$^+$, $P < 0.001$; FoxP3$^+$, $P = 0.034$; Student t test), however, this was not the case for peritumoral tissues (CD8$^+$, $P = 0.441$; FoxP3$^+$, $P = 0.017$; Student t test). **D,** Ratios of peri- to intratumoral CD8$^+$ TILs were calculated for all cases and evaluated by histogram and whisker plot (left). Data were then divided into three groups based on quartiles, and plotted by line graph (CD8$^+$ count, middle), and box and whisker plots (αSMA area index, right; $^*P < 0.05$, Tukey test with ANOVA). **E,** Ratios for peri- to intratumoral FoxP3$^+$ TILs were analyzed as for CD8$^+$ TILs. The opposite pattern to that seen for CD8$^+$ TILs for αSMA area index was observed ($^*P < 0.05$; Tukey test with ANOVA).

assessed using a bioluminescent imaging system (IVIS) every 4 days (Fig. 4A). Quantitative analysis of luciferase activity showed that the progression of Colon26-luc+NIH/3T3 tumors was significantly faster than Colon26-luc tumors, in both the BALB/c-*nu/nu* mice ($P < 0.05$, day 16) and the BALB/c mice ($P < 0.05$, day 12; and $P < 0.001$, day 16; Fig. 4B and C). Moreover, the luciferase activity in the Colon26-luc+NIH/3T3 group was 1.2 to 1.3 times higher than in the Colon26-luc group by day 16 in BALB/c-*nu/nu* mice, and 2.5 to 3.0 times higher in BALB/c mice (Fig. 4D). Therefore, the tumor progression ratio of the Colon26-luc+NIH/3T3 group to the Colon26-luc group was demonstrated more strongly in BALB/c, which are immunocompetent mice, than in BALB/c-n*u/nu* mice. In BALB/c mice, IHC showed that $CD8^+$ TIL numbers were lower in tumors from the Colon26-luc+NIH/3T3 group (in which numerous fibroblasts overexpressing αSMA were also detected), as compared with Colon26-luc group ($P = 0.0474$). In contrast, $FoxP3^+$ TIL numbers increased ($P = 0.251$), thus showing the same trend as in our clinical analysis (Fig. 4E). Thus, these results suggest that CAFs accelerate tumor immunosuppression by regulating TILs in intratumoral tissues and promoting tumor progression.

Elevated expression of IL6 in the tumor microenvironment

Next, we performed *in vitro* experiments to address the physiological basis of the observed TIL regulation by CAFs. First, we evaluated the expression level of TGFβ, which is known as a key tumor immunosuppressive cytokine. However, we found that not only CAFs, but also cancer cells, released TGFβ at high levels (Supplementary Fig. S3A and S3B). We then evaluated the involvement of other cytokines using a multicytokine array. Before the array, we first confirmed that NIH/3T3 normal fibroblasts acquired a CAF phenotype (i.e., overexpressed αSMA), when cultured in conditioned medium from Colon26 cancer cells, using immunofluorescent microscopy and Western blotting (Fig. 5A). Subsequently, we collected the supernatants from cancer cells cultured alone (Colon26 or SCCVII) as a control and the coculture of those cancer cells and NIH/3T3 fibroblasts, and measured the level of cytokines using the array (Supplementary Fig. S3C). The results demonstrated that the level of IL6 in cocultured supernatants was more than five times higher than in supernatants from cancer cells cultured alone. Therefore, we focused on IL6 and quantified this cytokine by ELISA in the supernatants from Colon26 and NIH/3T3 cells under various conditions (Fig. 5B). Colon26 or NIH/3T3 cells cultured alone released IL6, but the concentration was quite low. Meanwhile, cocultures of Colon26 and NIH/3T3 secreted higher concentrations of IL6. Furthermore, the concentration of IL6 increased as the number of NIH/3T3 cells seeded increased ($P < 0.001$, among all experimental groups). In contrast, the seeding density of Colon26 cells did not significantly affect the levels of IL6 in the supernatant, suggesting that it is CAFs that release IL6 at high levels, rather than cancer cells. We also confirmed that IL6 was still secreted at high levels when cells were cultured without direct contact (Fig. 5C). Various coculture combinations were tested between other mouse-derived cancer lines (4T1, SCCVII, and Pan02) and mouse-derived fibroblasts (MEF and BALBc/3T3; Fig. 5D). The trend to increase IL6 secretion as the result of coculture was observed for most of the combinations.

Finally, we repeated these experiments using four human esophageal cancer cell lines (TE1, TE4, TE8, and OE33) and three human fibroblast lines (FEF3, WI-38, and NHLF). As with the murine cells, the concentration of IL6 released by human CAFs activated by human cancer cells was significantly higher than seen with cancer cells alone or nonactivated fibroblasts (Supplementary Fig. S4). Furthermore, we checked the level of IL6 in cultured supernatants from several types of cancer cells, colon cancer (DLD-1), pancreatic cancer (Panc-1), and breast cancer (MCF-7) under the condition of cancer alone or coculture with several representative fibroblasts. High concentrations of IL6 in cocultured supernatants were detected under almost all conditions (Fig. 5E). These data suggest that under baseline conditions, cancer cells or normal fibroblasts release low levels of IL6; however, both mouse and human CAFs activated by cancer cells secrete high levels of IL6.

IL6 promotes tumor growth and immunosuppression *in vivo*

We next examined whether high levels of IL6 in intratumoral tissues cause immunosuppression *in vivo*. We used the murine-derived Colon26 cancer cells, and injected them into BALB/c and BALB/c-*nu/nu* mice subcutaneously. To mimic a high level of IL6 in intratumoral tissues, recombinant mouse IL6 was injected into the subcutaneous tumors directly every 3 days. The results demonstrated that in BALB/c-*nu/nu* mice, IL6 had a trend toward an additive effect, although this was not significant (Fig. 6A). However, in BALB/c mice, IL6 had a significantly additive effect and was associated with significantly greater tumor growth (Fig. 6B and C) and tumor weight gain (data not shown) compared with untreated tumors. Furthermore, with respect to tumor immunity, IHC demonstrated that the number of $CD8^+$ TILs in the Colon26+IL6 group was lower than in the Colon26 group (Fig. 6D). In contrast, there were higher numbers of $FoxP3^+$ TILs in the Colon26+IL6 group compared with the Colon26 group (Fig. 6E). Quantification of both $CD8^+$ and $FoxP3^+$ TILs revealed significant differences between the Colon26 and Colon26+IL6 groups (*, $P < 0.001$). It was also confirmed by IHC that the local IL6 concentration of the Colon26+IL6 group was indeed higher as intended (Fig. 6F). We also performed the same experiment using the pancreatic cancer cell line Pan02 in C57BL/6 mice. The same trends were observed as above, with the exception of quantification of $CD8^+$ TILs by IHC (Fig. 6G). Furthermore, we performed this experiment using the dermal squamous cell carcinoma cell line SCCVII in C3H/HeJ mice as a substitute for esophageal squamous cell carcinoma (Supplementary Fig. S5). Although significance was not demonstrated in tumor growth among both groups, the implantation rate of the xenograft in the IL6 group was obviously increased as compared with the control group (100% vs. 67%). Furthermore, IHC demonstrated that $CD8^+$ TILs were lower, whereas $FoxP3^+$ TILs were significantly higher in the SCCVII+IL6 group, which indicates immunosuppressive conditions. These results suggest that IL6 promotes tumor growth and immunosuppression by regulating $CD8^+$ or $FoxP3^+$ lymphocytes in intratumoral tissues.

Finally, to evaluate the reversibility of CAF-induced tumor immunosuppression via IL6, we performed *in vivo* experiments using murine Colon26 cells and BALB/c mice. Three tumor groups were compared; cancer cells alone (Colon26), cocultured cancer cells and fibroblasts (Colon26+NIH/3T3), and cocultured cells treated with anti-IL6 antibody (Colon26+NIH/3T3+anti-IL6 antibody). The results showed that the accelerated growth observed in cocultured tumors (*, $P < 0.05$) was significantly reduced by IL6 blockade (*, $P < 0.05$; Fig. 6H). The same trend was seen in regard to tumor weights (data not shown).

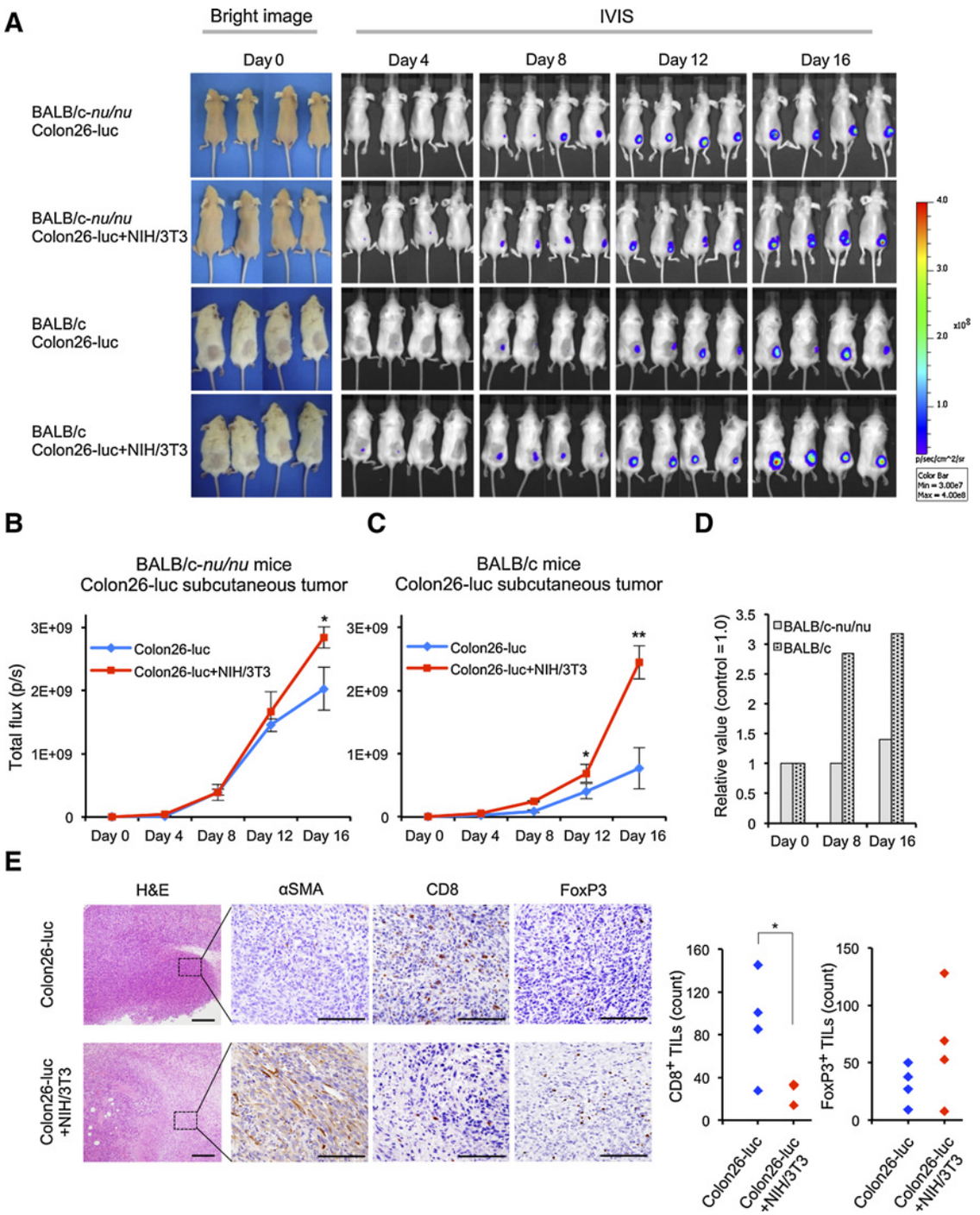

Figure 4.

CAFs promote tumor growth by regulating TILs *in vivo*. **A,** IVIS imaging of subcutaneous tumors of Colon26-luc cells alone, or Colon26-luc cells cocultured with NIH/3T3 fibroblasts, in BALB/c-*nu/nu* mice and BALB/c mice. **B,** Quantitative luciferin activities are shown for BALB/c-*nu/nu* mice (mean ± SEM; $^{*}P < 0.05$, day 16; Student *t* test). **C,** Quantitative analysis for BALB/c mice (mean ± SEM; $^{*}P < 0.05$, day 12; $^{**}P < 0.001$, day 16; Student *t* test). **D,** Relative progression of tumor growth in the coculture and control groups (Colon26-luc/Colon26-luc+NIH/3T3 tumors; **E**) IHC of CD8, FoxP3, and αSMA in BALB/c mice. Increased αSMA staining and FoxP3^{+} TILs, and decreased CD8^{+} TILs were observed in Colon26-luc+NIH/3T3 tumors (left). The number of CD8^{+} and FoxP3^{+} TILs in each sample is also plotted (right), showing a significantly lower number of CD8^{+} TILs in Colon26-luc+NIH/3T3 tumors ($^{*}P = 0.0474$, Tukey test with ANOVA), and a trend toward greater numbers of FoxP3^{+} TILs ($P = 0.251$, Tukey test with ANOVA). Scale bars: 200 μm (HE), 100 μm (IHC).

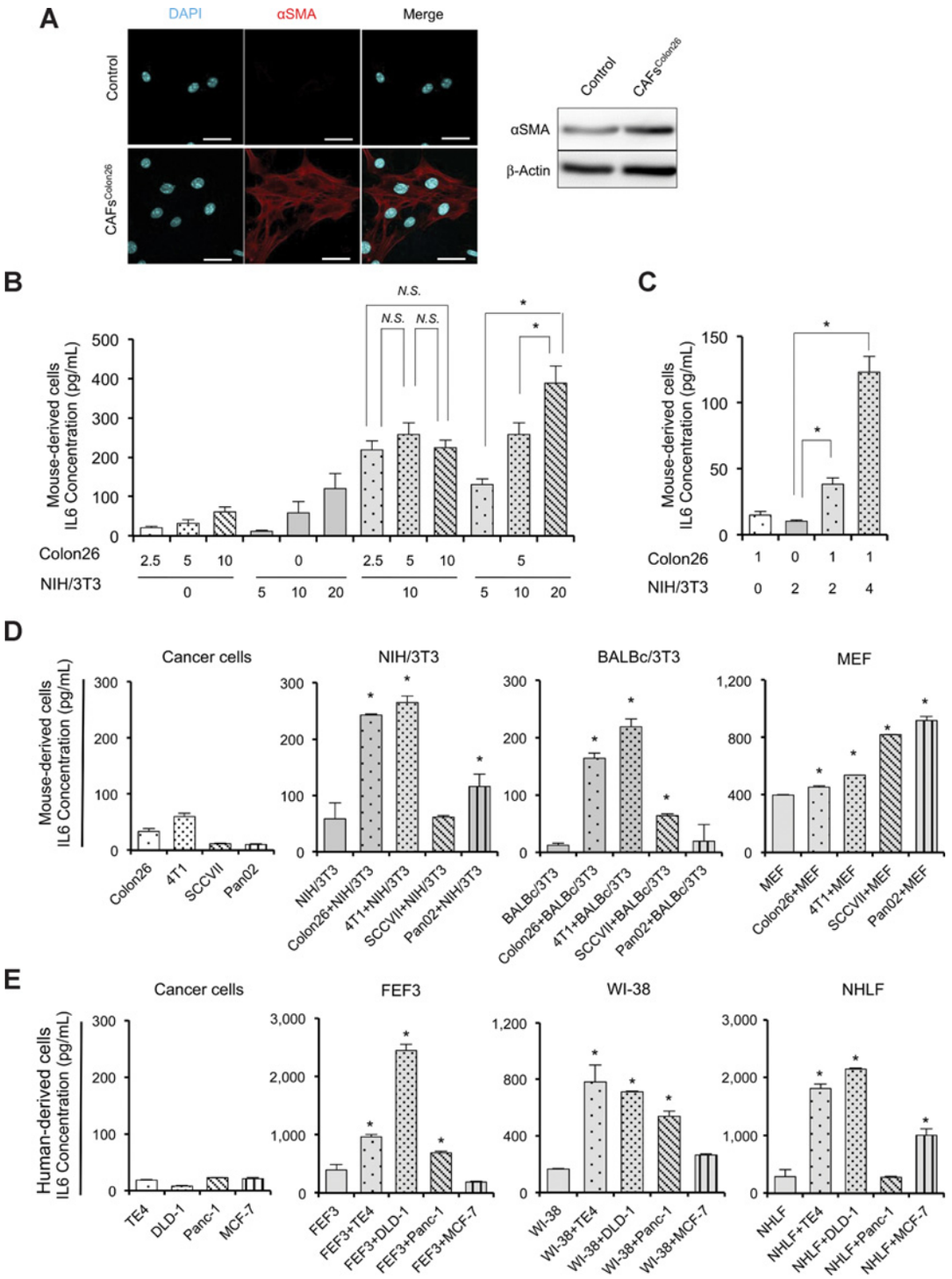

Figure 5.

Fibroblasts and cancer cells cooperate to promote the release of IL6. **A,** Immunofluorescent microscopy showed higher expression of αSMA in activated fibroblasts, stimulated by conditioned medium from Colon26 cells. Western blots showed higher expression of αSMA in CAFs vs. nonactivated fibroblasts. Scale bars: 50 μm. **B,** Quantification of IL6 secretion by ELISA. Cancer cells (Colon26) and normal fibroblasts (NIH/3T3) secreted IL6 in a seeding density-dependent manner ($\times 10^4$ cells). Under coculture conditions, IL6 secretion was significantly increased in a CAF-seeding density-dependent manner. **C,** Quantification of IL6 secretion from fibroblasts ($\times 10^4$ cells) using conditioned medium from Colon26 cells (1.0×10^4 cells) cultured in isolation, to evaluate stimulation under noncontact conditions. **D,** The stimulation of IL6 secretion using other types of cancer cells and fibroblasts was evaluated. Some of these lines had a high baseline level of IL6 secretion, such as 4T1 or MEF. However, most fibroblasts were stimulated by coculture with cancer cells to release IL6 excrete high levels. **E,** Quantification of IL6 secretion by human cells was investigated. The same trend was observed as with mouse-derived cells (panels **B–E:** data represent mean ± SD; $^*P < 0.05$, Tukey test with ANOVA; NS, not significant).

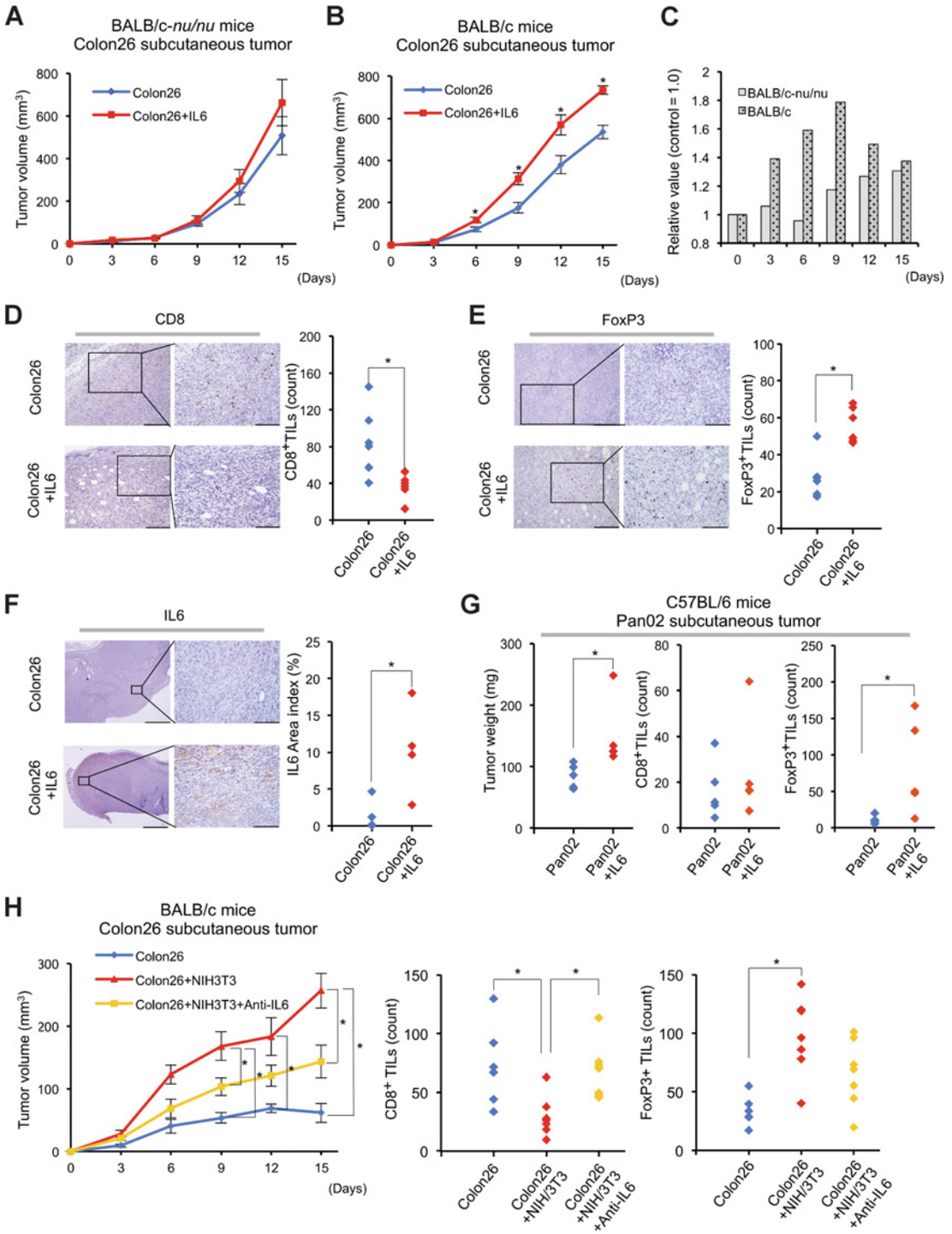

Figure 6.

IL6 accelerates tumor growth and immunosuppression by regulating TILs *in vivo*. **A** and **B,** Growth of subcutaneous tumors inoculated in BALB/c ($n = 6$, in each group) or BALB/c-*nu/nu* mice ($n = 5$, in each group) with or without IL6 injection was observed (mean ± SEM; $^*P < 0.05$; Student *t* test). **C,** Comparison of tumor progression in IL6-treated animals relative to untreated animals. **D,** IHC and quantification of $CD8^+$ TILs at high magnification (400×; $^*P < 0.001$, Student *t* test). **E,** IHC and quantification of $FoxP3^+$ TILs at high magnification (400×; $^*P < 0.001$, Student *t* test). **D** and **E,** Scale bars: 200 μm (200×), 100 μm (400×). **F,** IHC and quantification of the IL6 area index at high magnification (400×; $^*P < 0.001$, Student *t* test). Scale bars: 1 mm (40×), 100 μm (400×). **G,** Pan02 subcutaneous tumors in C57BL/6 mice were evaluated and stained for $CD8^+$ and $FoxP3^+$ TILs by IHC. Evaluation of tumor weight and the number of TILs is shown for each group ($^*P < 0.05$, Student *t* test). **H,** Tumor growth assay using anti-IL6 antibody to block IL6 effects (left). Comparison with or without IL6 blockade in cocultured tumors ($n = 7$ mice in each group; mean ± SD; $^*P < 0.05$, Tukey test with ANOVA). Number of $CD8^+$ and $FoxP3^+$ TILs in each sample is shown for each of the three groups (middle and right). Significantly decreased $CD8^+$ TIL numbers in NIH/3T3 cocultured tumors, and their subsequent rescue by IL6 blockade is shown (middle; $^*P < 0.05$, Tukey test with ANOVA). The significantly increased $FoxP3^+$ TIL numbers in cocultured tumors ($^*P < 0.05$), also showed a trend to reversal by IL6 blockade ($P = 0.101$; Colon26+NIH/3T3 vs. Colon26+NIH/3T3+anti-IL6, Tukey test with ANOVA).

Furthermore, in terms of immune status, IL6 blockade remodeled the TIL population in the TME as expected, with a significant increase in $CD8^+$ TILs ($P = 0.031$) and a significant decrease in $FoxP3^+$ TILs ($P = 0.101$). Thus, we demonstrated that CAFs affect tumor immunosuppression by regulating $CD8^+$ and $FoxP3^+$ TILs in intratumoral tissues by a mechanism involving IL6. Targeting CAFs with anti-IL6 antibodies may therefore be a therapeutic strategy to improve tumor immunosuppression and contribute to tumor regression.

Discussion

In this study, we demonstrated that CAFs have a strong association with a population of TILs, which could lead to immunosuppressive conditions in the TME. These findings were consistent between *in vitro* and *in vivo* experiments, and in our analysis of clinical samples of esophageal cancer. Our data show that $CD8^+$ lymphocytes (cytotoxic T cells) and $FoxP3^+$ lymphocytes (regulatory T cells) are independent prognostic factors for esophageal cancer, but only with regard to their presence in intratumoral, not peritumoral tissues. Furthermore, CAFs have a significant correlation with $CD8^+$ or $FoxP3^+$ TILs in intratumoral tissues, suggesting that CAFs cooperate with cancer cells to control migration of TILs into the tumor. This raises questions as to whether it is the absolute number of TILs that is important (as opposed to their relative balance between the intra- and peritumoral tissues), and how the CAFs regulate the TIL population of the TME.

To address these questions, we analyzed the TIL ratio between the peri- and intratumoral sites. We found that a high ratio of peri- to intratumoral $CD8^+$ or low ratio of $FoxP3^+$ TILs tended to be associated with a high αSMA index, indicating that it is the CAFs that affect the peri- to intratumoral migration of those TILs (Fig. 3D and E; Supplementary Fig. S2). Another important finding of our study is the observation that CAFs stimulated by cancer cells release IL6 at high levels, and that IL6 may therefore coordinate the migration of TILs. TGFβ in the TME has been known to play an important role in both tumor progression (24) and tumor immunity. In our study, although the level of TGFβ in the co-culture system *in vitro* was found to be elevated, the cytokine is not specifically secreted by fibroblasts. Therefore, in our study, we focused on IL6, as CAFs are the major source of this cytokine.

IL6 is a well-known inflammatory cytokine and it has previously been reported that IL6 plays an important role in tumorigenesis, tumor proliferation, invasion, angiogenesis, and tumor immunosuppression via signaling pathways in the TME involving JAK/STAT, MEK, and AKT (41–43). In our study, we artificially created a high level of IL6 in intratumoral tissues by injection of the cytokine directly into the tumor site. No significant difference in tumor growth was detected in the immune-deficient BALB/c-*nu/nu* mice in response to IL6, whereas significantly higher tumor growth was demonstrated in BALB/c mice, which are immune-competent. Furthermore, IL6 blockade decreased tumor growth, and remodeled the TIL population in a direction that would be expected to improve antitumor immunity. We confirmed using surgically-resected specimens that IL6 expression *in vivo* coincides with the location of αSMA^+ stromal cells (Supplementary Fig. S6). High concentrations of IL6 may promote an immunosuppressive TME, as demonstrated by lower numbers of $CD8^+$ and higher numbers of $FoxP3^+$ TILs in CAF-rich tumors.

However, in general, IL6 inhibits Treg differentiation induced by TGFβ from naive T cells (44), which does not explain our results. We hypothesize that T-cell metabolism is strongly related to the distinctive tumor microenvironment, which is under hypoxia conditions caused by CAFs and IL6 (45). It is known that hypoxia-inducible factor 1α (HIF1α) is controlled by oxygen level and is stabilized under hypoxic conditions (45–47). It has also been reported that CAFs and IL6 induce reactive oxygen species (ROS), and ROS affect hypoxic conditions (48, 49). In effector T cells, stabilized HIF1α results in activation of glycolytic metabolism. In tumor cells, the enhanced conversion of glucose to lactate was revealed by the Warburg effect (50). As a result of glucose deficiency, effector T cells compete with tumor cells for glucose within the tumor niche (51, 52), and $CD8^+$ T cells tend to decrease under such conditions. However, Treg cells are highly dependent on mitochondrial metabolism having the flexibility to use oxidized lipid or glucose as a fuel source (51, 52). Thus, Treg cells are tolerant to hypoxic conditions and appear to increase under these conditions. Furthermore, another group reported that ROS themselves induce Treg (46). From the above considerations, it is thought that lower $CD8^+$ T cells and higher $FoxP3^+$ T cells could be present under hypoxic tumor conditions. Conversely to intratumoral conditions, the activity of $CD8^+$ T cells is thought to be maintained in an aerobic environment in peritumoral tissues. Our hypothesis is supported by the observation that HIF1α and carbonic anhydrase IX (CAIX), which is a major downstream target of HIF1α, were overexpressed together with IL6 expression in cases with high αSMA by IHC (Supplementary Fig. S7). We previously reported that CAFs secreted vascular endothelial growth factor, which also promotes hypoxic conditions (24). Thus, from the viewpoint of tumor metabolism and hypoxia, there may be a different role for IL6 in tumor immunity in the tumor microenvironment as compared with the systemic non-tumor microenvironment.

Understanding the regulation of TILs by CAFs may improve conventional immune therapies (5–8). Currently, these strategies are focused on activating preexisting immunity (16). Clinical evidence has demonstrated that immune checkpoint inhibitors are more effective in inflamed tumors, which are characterized as having high $CD8^+$ T-cell density (28, 53). Meanwhile, efficacy has been limited in cases where $CD8^+$ TILs in intratumoral tissues are low in number. In such cases, combination therapy strategies may be envisaged to both stimulate preexisting immune cell function and antitumor T-cell infiltration (17). It is clear that CAFs are a major source of regulation of $CD8^+$ cytotoxic T cells within the TME. Therefore, controlling CAFs presents the possibility of improving the immunosuppressive microenvironment for immune checkpoint inhibitors. To this end, a recent report has confirmed that IL6 and PD-L1 antibody blockade combination therapy reduces tumor progression in murine pancreatic cancer models (41). In addition, the trafficking of $CD8^+$ T cells into intratumoral tissues may prove critical in improving the efficacy of other immune therapies, such as CAR-T-cell therapy and cancer vaccine therapies (10, 16).

It should be recognized, however, that targeting CAFs therapeutically has some challenges. First, CAFs may be derived from a number of cell types, such as fibroblasts, myeloid cells, epithelial cells, and adipocytes. Second, there are no specific markers to identify CAFs. In this study, however, we demonstrated that IL6 blockade resulted in improved tumor immunity, and given that IL6 blocking antibodies are already approved by the FDA, such an approach to restore an immunosuppressive TME may be a viable strategy in the clinic. Despite this, the development of more

radical therapies directly targeting CAFs may still be required in the future.

Our study has some limitations. First, we evaluated the location of $CD8^+$ and $FoxP3^+$ lymphocytes by IHC, rather than evaluating their functionality. T-cell exhaustion was not examined, and in regard to $FoxP3^+$ lymphocytes, Treg functionality was not assessed. It should be considered whether IHC with the single $FoxP3^+$ would be enough for evaluation of Treg. Furthermore, it is unclear whether the changes in both TILs are caused by trafficking or selection. It is reported that trafficking of Treg cells in the tumor is caused by the chemokine CCL22 produced by tumor-associated macrophages and tumor cells (54); therefore, verification of T-cell trafficking by CAFs is necessary. In addition, further experiments are necessary to confirm our hypothesis regarding the correlation between IL6 and T-cell metabolism. Finally, the investigation of effects from T cells to CAFs is also another issue, which is in the opposite direction as demonstrated in this study. Other groups have reported that effector T cells control stroma-mediated chemoresistance by altering the metabolism of CAFs in the tumor microenvironment (55). Thus, further investigation is required regarding the crosstalk between T-cell activation and suppression, and CAF signaling.

In conclusion, we have described a role for CAFs in modulating tumor immunity in esophageal cancer, in particular in regard to the intratumoral migration of TILs. CAFs remodel the immunosuppressive TIL population of the TME, via the secretion of high levels of IL6. Blockade of IL6 signaling or therapies directly targeting CAFs could improve T-cell trafficking, migration, and tumor immunosuppression, and thus improve the prognosis of patients with many different types of cancer, including esophageal cancer.

Disclosure of Potential Conflicts of Interest

No potential conflicts of interest were disclosed.

Authors' Contributions

Conception and design: K. Noma, T. Ohara, T. Ninomiya, Y. Shirakawa, T. Fujiwara
Development of methodology: T. Kato, K. Noma, T. Ninomiya
Acquisition of data (provided animals, acquired and managed patients, provided facilities, etc.): T. Kato, H. Kashima, Y. Katsura, S. Komoto, R. Katsube
Analysis and interpretation of data (e.g., statistical analysis, biostatistics, computational analysis): T. Kato, K. Noma, T. Ninomiya
Writing, review, and/or revision of the manuscript: K. Noma, T. Fujiwara
Administrative, technical, or material support (i.e., reporting or organizing data, constructing databases): T. Kato, K. Noma, H. Sato, H. Tazawa, Y. Shirakawa
Study supervision: K. Noma, Y. Shirakawa, T. Fujiwara

Acknowledgments

We are grateful to Ms. Tomoko Sueishi and Ms. Tae Yamanishi for their technical assistance, and also to Dr. Shingo Eikawa and Heiichiro Udono (Department of Immunology, Okayama University, Okayama, Japan) for useful discussions. This work was supported by grants-in-aid from the Ministry of Education, Science, and Culture, Japan; and Grants from the Ministry of Health and Welfare, Japan.

The costs of publication of this article were defrayed in part by the payment of page charges. This article must therefore be hereby marked *advertisement* in accordance with 18 U.S.C. Section 1734 solely to indicate this fact.

Received January 18, 2018; revised May 8, 2018; accepted June 13, 2018; published first June 19, 2018.

References

1. Zhang Y. Epidemiology of esophageal cancer. World J Gastroenterol 2013;19:5598–606.
2. Gubin MM, Zhang X, Schuster H, Caron E, Ward JP, Noguchi T, et al. Checkpoint blockade cancer immunotherapy targets tumour-specific mutant antigens. Nature 2014;515:577–81.
3. Schumacher TN, Schreiber RD. Neoantigens in cancer immunotherapy. Science 2015;348:69–74.
4. Snyder A, Makarov V, Merghoub T, Yuan J, Zaretsky JM, Desrichard A, et al. Genetic basis for clinical response to CTLA-4 blockade in melanoma. N Engl J Med 2014;371:2189–99.
5. Brahmer JR, Tykodi SS, Chow LQ, Hwu WJ, Topalian SL, Hwu P, et al. Safety and activity of anti-PD-L1 antibody in patients with advanced cancer. N Engl J Med 2012;366:2455–65.
6. Hodi FS, O'Day SJ, McDermott DF, Weber RW, Sosman JA, Haanen JB, et al. Improved survival with ipilimumab in patients with metastatic melanoma. N Engl J Med 2010;363:711–23.
7. Leach DR, Krummel MF, Allison JP. Enhancement of antitumor immunity by CTLA-4 blockade. Science 1996;271:1734–6.
8. Wolchok JD, Kluger H, Callahan MK, Postow MA, Rizvi NA, Lesokhin AM, et al. Nivolumab plus ipilimumab in advanced melanoma. N Engl J Med 2013;369:122–33.
9. Eikawa S, Nishida M, Mizukami S, Yamazaki C, Nakayama E, Udono H. Immune-mediated antitumor effect by type 2 diabetes drug, metformin. Proc Natl Acad Sci U S A 2015;112:1809–14.
10. Wang LC, Lo A, Scholler J, Sun J, Majumdar RS, Kapoor V, et al. Targeting fibroblast activation protein in tumor stroma with chimeric antigen receptor T cells can inhibit tumor growth and augment host immunity without severe toxicity. Cancer Immunol Res 2014;2:154–66.
11. Jacquelot N, Roberti MP, Enot DP, Rusakiewicz S, Ternes N, Jegou S, et al. Predictors of responses to immune checkpoint blockade in advanced melanoma. Nat Commun 2017;8:592.
12. Dushyanthen S, Teo ZL, Caramia F, Savas P, Mintoff CP, Virassamy B, et al. Agonist immunotherapy restores T cell function following MEK inhibition improving efficacy in breast cancer. Nat Commun 2017;8:606.
13. Zhu J, Powis de Tenbossche CG, Cane S, Colau D, van Baren N, Lurquin C, et al. Resistance to cancer immunotherapy mediated by apoptosis of tumor-infiltrating lymphocytes. Nat Commun 2017;8:1404.
14. Predina J, Eruslanov E, Judy B, Kapoor V, Cheng G, Wang LC, et al. Changes in the local tumor microenvironment in recurrent cancers may explain the failure of vaccines after surgery. Proc Natl Acad Sci U S A 2013;110:E415–24.
15. Feig C, Jones JO, Kraman M, Wells RJ, Deonarine A, Chan DS, et al. Targeting CXCL12 from FAP-expressing carcinoma-associated fibroblasts synergizes with anti-PD-L1 immunotherapy in pancreatic cancer. Proc Natl Acad Sci U S A 2013;110:20212–7.
16. Herbst RS, Soria JC, Kowanetz M, Fine GD, Hamid O, Gordon MS, et al. Predictive correlates of response to the anti-PD-L1 antibody MPDL3280A in cancer patients. Nature 2014;515:563–7.
17. Kim JM, Chen DS. Immune escape to PD-L1/PD-1 blockade: seven steps to success (or failure). Ann Oncol 2016;27:1492–504.
18. Salmon H, Franciszkiewicz K, Damotte D, Dieu-Nosjean MC, Validire P, Trautmann A, et al. Matrix architecture defines the preferential localization and migration of T cells into the stroma of human lung tumors. J Clin Invest 2012;122:899–910.
19. Joyce JA, Fearon DT. T cell exclusion, immune privilege, and the tumor microenvironment. Science 2015;348:74–80.
20. Junttila MR, de Sauvage FJ. Influence of tumour micro-environment heterogeneity on therapeutic response. Nature 2013;501:346–54.
21. Mezawa Y, Orimo A. The roles of tumor- and metastasis-promoting carcinoma-associated fibroblasts in human carcinomas. Cell Tissue Res 2016;365:675–89.

22. Motz GT, Santoro SP, Wang LP, Garrabrant T, Lastra RR, Hagemann IS, et al. Tumor endothelium FasL establishes a selective immune barrier promoting tolerance in tumors. Nat Med 2014;20:607–15.
23. Augsten M. Cancer-associated fibroblasts as another polarized cell type of the tumor microenvironment. Front Oncol 2014;4:62.
24. Noma K, Smalley KS, Lioni M, Naomoto Y, Tanaka N, El-Deiry W, et al. The essential role of fibroblasts in esophageal squamous cell carcinoma-induced angiogenesis. Gastroenterology 2008;134:1981–93.
25. Spaeth EL, Dembinski JL, Sasser AK, Watson K, Klopp A, Hall B, et al. Mesenchymal stem cell transition to tumor-associated fibroblasts contributes to fibrovascular network expansion and tumor progression. PLoS One 2009;4:e4992.
26. Kraman M, Bambrough PJ, Arnold JN, Roberts EW, Magiera L, Jones JO, et al. Suppression of antitumor immunity by stromal cells expressing fibroblast activation protein-alpha. Science 2010;330:827–30.
27. Yang X, Lin Y, Shi Y, Li B, Liu W, Yin W, et al. FAP promotes immunosuppression by cancer-associated fibroblasts in the tumor microenvironment via STAT3-CCL2 signaling. Cancer Res 2016;76:4124–35.
28. Hegde PS, Karanikas V, Evers S. The where, the when, and the how of immune monitoring for cancer immunotherapies in the era of checkpoint inhibition. Clin Cancer Res 2016;22:1865–74.
29. Arigami T, Uenosono Y, Ishigami S, Matsushita D, Hirahara T, Yanagita S, et al. Decreased density of CD3+ tumor-infiltrating lymphocytes during gastric cancer progression. J Gastroenterol Hepatol 2014;29:1435–41.
30. Liu F, Lang R, Zhao J, Zhang X, Pringle GA, Fan Y, et al. CD8(+) cytotoxic T cell and FOXP3(+) regulatory T cell infiltration in relation to breast cancer survival and molecular subtypes. Breast Cancer Res Treat 2011;130: 645–55.
31. Rathore AS, Kumar S, Konwar R, Makker A, Negi MP, Goel MM. CD3+, CD4+ & CD8+ tumour infiltrating lymphocytes (TILs) are predictors of favourable survival outcome in infiltrating ductal carcinoma of breast. Indian J Med Res 2014;140:361–9.
32. Salgado R, Denkert C, Demaria S, Sirtaine N, Klauschen F, Pruneri G, et al. The evaluation of tumor-infiltrating lymphocytes (TILs) in breast cancer: recommendations by an International TILs Working Group 2014. Ann Oncol 2015;26:259–71.
33. Teng F, Mu D, Meng X, Kong L, Zhu H, Liu S, et al. Tumor infiltrating lymphocytes (TILs) before and after neoadjuvant chemoradiotherapy and its clinical utility for rectal cancer. Am J Cancer Res 2015;5:2064–74.
34. Yagi T, Baba Y, Ishimoto T, Iwatsuki M, Miyamoto Y, Yoshida N, et al. PD-L1 expression, tumor-infiltrating lymphocytes, and clinical outcome in patients with surgically resected esophageal cancer. Published Online: 2017. Ann Surg.
35. Smit JK, Muijs CT, Burgerhof JG, Paardekooper G, Timmer PR, Muller K, et al. Survival after definitive (chemo)radiotherapy in esophageal cancer patients: a population-based study in the north-East Netherlands. Ann Surg Oncol 2013;20:1985–92.
36. Sudo T, Nishida R, Kawahara A, Saisho K, Mimori K, Yamada A, et al. Clinical impact of tumor-infiltrating lymphocytes in esophageal squamous cell carcinoma. Ann Surg Oncol 2017;24:3763–70.
37. Wang J, Jia Y, Wang N, Zhang X, Tan B, Zhang G, et al. The clinical significance of tumor-infiltrating neutrophils and neutrophil-to-CD8+ lymphocyte ratio in patients with resectable esophageal squamous cell carcinoma. J Transl Med 2014;12:7.
38. Zhu Y, Li M, Mu D, Kong L, Zhang J, Zhao F, et al. CD8+/FOXP3+ ratio and PD-L1 expression associated with survival in pT3N0M0 stage esophageal squamous cell cancer. Oncotarget 2016;7:71455–65.
39. Chen DS, Mellman I. Oncology meets immunology: the cancer-immunity cycle. Immunity 2013;39:1–10.
40. Ogasawara K. 8. Revised "Ethical Guidelines for Medical and Health Research Involving Human Subjects". Nihon Hoshasen Gijutsu Gakkai Zasshi 2017;73:397–402.
41. Mace TA, Shakya R, Pitarresi JR, Swanson B, McQuinn CW, Loftus S, et al. IL-6 and PD-L1 antibody blockade combination therapy reduces tumour progression in murine models of pancreatic cancer. Gut 2016;67:320–32.
42. Scheller J, Chalaris A, Schmidt-Arras D, Rose-John S. The pro- and anti-inflammatory properties of the cytokine interleukin-6. Biochim Biophys Acta 2011;1813:878–88.
43. Zhang Y, Yan W, Collins MA, Bednar F, Rakshit S, Zetter BR, et al. Interleukin-6 is required for pancreatic cancer progression by promoting MAPK signaling activation and oxidative stress resistance. Cancer Res 2013;73:6359–74.
44. Kimura A, Kishimoto T. IL-6: regulator of Treg/Th17 balance. Eur J Immunol 2010;40:1830–5.
45. Gorlach A, Dimova EY, Petry A, Martinez-Ruiz A, Hernansanz-Agustin P, Rolo AP, et al. Reactive oxygen species, nutrition, hypoxia and diseases: problems solved? Redox Biol 2015;6:372–85.
46. Kraaij MD, Savage ND, van der Kooij SW, Koekkoek K, Wang J, van den Berg JM, et al. Induction of regulatory T cells by macrophages is dependent on production of reactive oxygen species. Proc Natl Acad Sci U S A 2010; 107:17686–91.
47. Jin MS, Lee H, Park IA, Chung YR, Im SA, Lee KH, et al. Overexpression of HIF1alpha and CAXI predicts poor outcome in early-stage triple negative breast cancer. Virchows Arch 2016;469:183–90.
48. Chan JS, Tan MJ, Sng MK, Teo Z, Phua T, Choo CC, et al. Cancer-associated fibroblasts enact field cancerization by promoting extratumoral oxidative stress. Cell Death Dis 2017;8:e2562.
49. Sung JY, Hong JH, Kang HS, Choi I, Lim SD, Lee JK, et al. Methotrexate suppresses the interleukin-6 induced generation of reactive oxygen species in the synoviocytes of rheumatoid arthritis. Immunopharmacology 2000;47:35–44.
50. Kim JW, Dang CV. Cancer's molecular sweet tooth and the Warburg effect. Cancer Res 2006;66:8927–30.
51. Chang CH, Qiu J, O'Sullivan D, Buck MD, Noguchi T, Curtis JD, et al. Metabolic competition in the tumor microenvironment is a driver of cancer progression. Cell 2015;162:1229–41.
52. Galgani M, De Rosa V, La Cava A, Matarese G. Role of metabolism in the immunobiology of regulatory T cells. J Immunol 2016;197:2567–75.
53. Ji RR, Chasalow SD, Wang L, Hamid O, Schmidt H, Cogswell J, et al. An immune-active tumor microenvironment favors clinical response to ipilimumab. Cancer Immunol Immunother 2012;61:1019–31.
54. Curiel TJ, Coukos G, Zou L, Alvarez X, Cheng P, Mottram P, et al. Specific recruitment of regulatory T cells in ovarian carcinoma fosters immune privilege and predicts reduced survival. Nat Med 2004;10: 942–9.
55. Wang W, Kryczek I, Dostal L, Lin H, Tan L, Zhao L, et al. Effector T cells abrogate stroma-mediated chemoresistance in ovarian cancer. Cell 2016; 165:1092–105.